第 34 卷第 1 期
2015 年 2 月

红 外 与 毫 米 波 学 报
J. Infrared Millim. Waves

Vol. 34, No. 1
February, 2015

文章编号:1001 - 9014(2015)01 - 0001 - 05

DOI:10.3724/SP. J. 1010. 2015. 00001

A 270 GHz high performance waveguide detector utilizing a zero-bias Schottky diode

ZHANG Jian-Jun[1,2], ZHOU Jing-Tao[1*], YANG Cheng-Yue[1], TIAN Zhong[2], JIN Zhi[1*]

(1. Department of Microwave Devices and Integrated Circuits, Institute of Microelectronics, Chinese Academy of Sciences, Beijing 100029, China;
2. Research Institute of Electronic Science and Technology, University of Electronic Science and Technology of China, Chengdu 611731, China)

Abstract: According to the structure of the InP diode, 3-D high frequency simulate software was adopted to create accurate physical model and matching circuits of the diode. Harmonic balance simulation was used to simulate the whole circuits. Based on this type of InP Schottky diode, a 270 GHz zero bias detector was designed and measured for the first time in China. The measured responsivity is near 1600 V/W at 260 GHz, as well as 1400 V/W over 260 ~ 280 GHz typically, which corresponds to typical noise equivalent power level (NEP) of 18 pW/ $Hz^{1/2}$. The measured and simulated results are highly similar, indicating that this solution has the advantages of accurate, simplified and easily optimized.

Key words: Terahertz, detector, InP Schottky barrier diode
PACS: 84.30.Qi

基于零偏置肖特基二极管的 270 GHz 高性能波导检波器

张建军[1,2], 周静涛[1*], 杨成樾[1], 田 忠[2], 金 智[1*]

(1. 中国科学院微电子研究所,北京 100029;
2. 电子科技大学电子科学技术研究院,四川 成都 611731)

摘要:根据 InP 二极管的物理结构,采用三维高频电磁仿真软件对其精确建模仿真,获得二极管的物理模型和匹配电路的精确参数,而后将此模型利用谐波平衡进行仿真设计. 最后,在此基础上采用 InP 肖特基二极管,设计制作并测试了国内首款 270 GHz 的零偏置检波器. 检波器的最大电压响应度为 1 600 V/W,在 260 ~ 280 GHz 范围内,电压响应的典型值为 1 400 V/W,其对应的等效噪声功率典型值为 18 pW/ $\sqrt{\text{Hz}}$. 实验结果与仿真结果比较吻合,其结果表明,设计方法较为精确,具有设计简单、优化方便等优点.

关 键 词:太赫兹;检波器;InP 肖特基二极管

中图分类号:TN722.7 **文献标识码**:A

Introduction

Terahertz covers the frequency band from infrared to millimeter waves. This electromagnetic spectrum is attractive because terahertz wave sources can be used for a variety of applications such as molecular spectroscopy, atmospheric remote sensing, scaled radar range systems, sensing and monitoring of chemical and biological molecules, etc.[1] With the development of terahertz technologies, there is pressing need of compact, high speed and highly sensitive detector for THz radiation which operated at room temperature. Conventional cryogenic bolometers are extremely sensitive by providing responsivity up to 105 V/W, and NEP about 10 ~ 13 pW/$Hz^{1/2}$. However, they have slow temporal response relatively. Pyroelectric (PE) detectors is considered as an exotic type of bolometer, which have long response time up to 1 ms relatively[2]. Schottky diode detector becomes a very effective way, which has shorter response time. In addition, In-

Received date: 2013 - 08 - 27, **revised date**: 2014 - 06 - 05 **收稿日期**:2013 - 08 - 27, **修回日期**:2014 - 06 - 05
Foundation items: Supported by the National Basic Research Program of China (2010CB327502) and the National Nature Science Foundation of China (61434006), (61106074)
Biography: ZHANG Jian-Jun(1987-), male, SiChuan, China, Post-Graduate. Research fields focus on microwave circuits design. E-mail: 070304015@163.com
* **Corresponding author**: E-mail: jinzhi@ime.ac.cn

GaAs/InP[3] appears to be very promising material system for the detection of millimeter and submillimeter waves. Compared with GaAs, InGaAs/InP Schottky barrier provides zero-bias detection ability (InP Schottky barrier diode have as lower forward turn-on voltage as 0.2 V, while the breakdown voltage is small). This property not only eliminates shot noise to improve crucially signal-to-noise ratio, but also simplifies the detection system[4]. In foreign countries, Schottky barrier zero bias detector based on InGaAs / InP has been developed much mature, represented by Virginia Diodes Inc (VDI). Their Schottky diode detectors use rectangular waveguide housings and the entire circuit is optimized for operation over the full single-moded waveguide band without any mechanical tuners. Their responsivity typically ranges from about 4 000 V/W at 100 GHz to 400 V/W at 900 GHz. In our country, the THz detector technology research is still at the infancy stage. Nanjing Electronic Devices Institute developed detectors based on GaAs Schottky diode, voltage sensitivity at 0.11 ~ 0.17 THz is 600 V/W typically[5]. Suzhou Nano developed quasi-optical detector based on GaN/AlGaN high electron mobility transistors, the voltage responsivity in the 800 ~ 1 100 GHz is greater than 3.6 kV/W, noise equivalent power is less than 40 pW/Hz$^{1/2}$[2]. However, Schottky barrier zero bias detector based on InGaAs / InP is barely not reported at present.

In this paper, a 270 GHz detector was designed base on the InP Schottky diode from Institute of Microelectronics of Chinese Academy of Sciences(IMCAS). All passive networks were analyzed by electromagnetic(EM) simulator. The non-linear behavior of the diode and optimization of the whole detector circuit were analyzed by Agilent's ADS, with the help of harmonic balance analysis(HBA).

1 Circuit design

An "divide and combine" co-simulation design approach is adopted, as shown in Fig. 1. Firstly, the structure of each module circuit realization is determined. In this design, a single InP Schottky diode is adopted as the core circuit of the detector. The schematic diagram and structure diagram are shown in Fig. 2. Secondly, according to the structure of circuit and the boundary conditions of the diode, the physical model is established by using the electromagnetic simulation software Ansoft's high frequency structure simulator(HFSS). Through the simulation, the S-parameter file is achieved. Moreover, harmonic balance analysis is used to determine the optimal input and output impedance of the circuit in the operating frequency. Thirdly, each part of the passive circuits is designed base on optimal impedance individually, such as input waveguide-microstrip transition, matching networks and so on. Finally, base on the optimal passive circuit network, the overall field module is established. The 3-port S-parameter is extracted and the circuit is re-optimized. The process was repeated until the performance meets the target.

1.1 Diode model design

In this paper, a single InP Schottky diode made by IMCAS was adopted. The cross section view of the InP

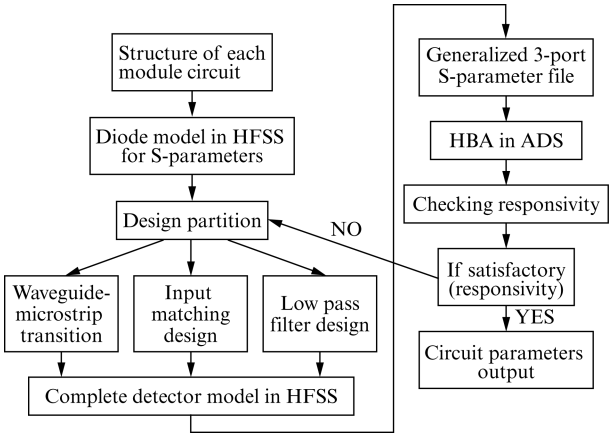

Fig. 1 Detector design flow chart
图1 检波器设计流程

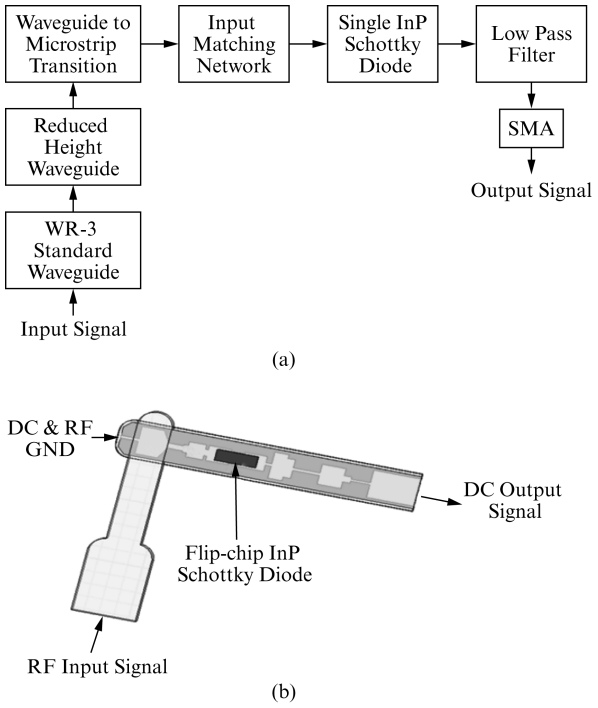

Fig. 2 (a) Schematic diagram of 270 GHz detector. (b) Structure of 270 GHz detector
图2 (a)270 GHz 检波器原理图(b)270 GHz 检波器结构图

Schottky diode is shown in Fig. 3(a). It's structure and material are depicted briefly as follows: a 50 μm thick semi-insulating SI-InP substrate serves as a supporting structure for diode. The epitaxial lattice matched $In_{0.53}Ga_{0.47}As$ structure include a 1.5 μm thick heavily doped n + InGaAs layer and a 0.2 μm thick n InGaAs layer above, the doping concentration of the two layers are 3×10^{19} cm^3 and 2×10^{17} cm^3, respectively. A 0.5 um thick SiO_2 layer is deposited on the n InGaAs layer to provide passivation and insulation. The ohmic contact is formed at the n + InGaAs layer by etching through the n InGaAs layer and depositing a Ti-Pt-Au metal[5]. Equivalent circuit of InP Schottky diode is shown in Fig. 3(b). The junction resistance R_j is very large which can be neglected. The junction capacitance, C_{j0}, is the zero-biased

junction capacitance. The diode series resistance, Rs, is a non-trivial parasitic element where power is dissipated. The total parasitic capacitance, C_p, is dependent on the diode material and geometry.

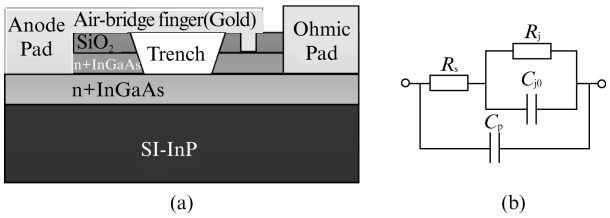

Fig. 3　(a) Cross section view of InP Schottky diode[7] (b) Equivalent circuit of InP Schottky diode

图 3　(a) InP 肖特基二极管截面图[7] (b) InP 肖特基二极管等效电路

The dimension of the diode is 0.24 mm × 0.11 mm × 0.05 mm (length, width and thickness, respectively), which can be comparable with operation wavelength. When operation frequency is high, the accurate model of the diode is fundamental for the detector design[1,5]. When establishing the 3-D model of the diode in HFSS, in order to shorten the simulation time, the diode parameters are taken with approximation as shown in Table 1. The n + InGaAs layer can be set as perfect conductor instead; other materials are modeled as lossless media. According to physics structure of the diode, the 3D model of the diode package is established shown in Fig. 4, in a flip-chip configuration. In the EM simulation, the active part of the diode is replaced by an internal coaxial or lump port[6-8]. In this way, the diode barrier (non-linear part) and diode parasitics (passive 3D part) can be separated. The result of the 3D model by EM simulation is imported to ADS in the form of S-parameter file and the internal ports are connected to non-linear diode model, which is modeled by SPICE parameters (C_{jo} = 9 fF, I_{sat} = 0.54 μA, R_S = 3.32 Ω, η = 1.185, C_p = 4 fF). By running HBA in ADS, the optimum impedances of detector can be achieved.

Table 1　Parameter values for the diode material

表 1　二极管材料参数

Material	Relative permittivity	Bulk conductivity (S/m)
n + InGaAs	–	PEC
n InGaAs	13.15	0
SiO2	4	0
InP	12.15	0

1.2　Linear analysis

All passive networks of the detector are analyzed and designed by HFSS. In order to reduce the solve space and simplify the design procedure, the structure is divided into the following parts: input waveguide to microstrip transition, input matching networks and low pass filter. In order to realize perfect match between the waveguide and microstrip, it is necessary to design the match network. This solution would keep the input signal energy transport through the input circuit to the diode as much as possible. The simulation result of the Waveguide-microstrip transition is shown in Fig. 5 (a).

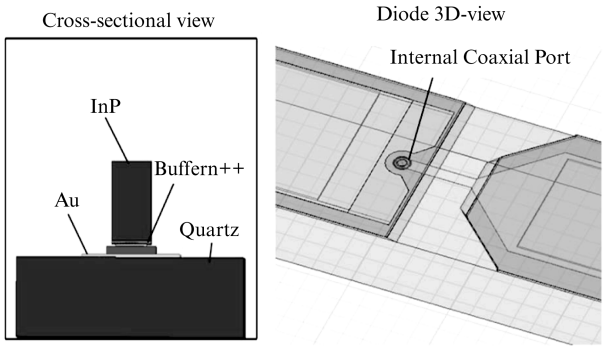

Fig. 4　Full 3D-Model used for electromagnetic simulation of the flip-chip mounted single diode

图 4　倒装安装的单二极管电磁场 3D 模型

To make the DC signal connects to the ground, as well as reduce the size, the height of the standard waveguide is decreased. The signal is coupled to the output port though probe, and transport to the diode. Fig. 5 (b) is the simulated result of the probe. From this, the input waveguide to microstrip transition makes input signal energy propagate well. As indicated in Fig. 6 (a), a low-pass filter is designed to isolate the detector signal (i. e. DC signal) from the RF signal. The filter adopts stepped impedance microstrip low pass filter. Due to parasitic band, the 1-dB cut-off frequency of the filter is 140 GHz. The simulated results of the low pass filter are presented in Fig. 6 (b), the low pass filter has band rejection about 20 dB among 260 ~ 280 GHz.

1.3　Detecting circuit optimization

The detecting circuit is fabricated on substrate of quartz with dielectric constant of 3.78, and thickness of

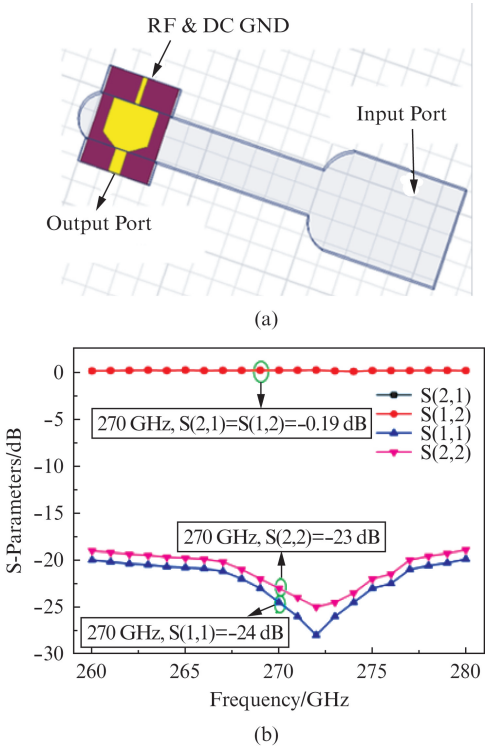

Fig. 5　The structure (a) and simulated result (b) of the input waveguide to microstrip transition

图 5　输入波导到微带过渡结构(a)和仿真结果(b)

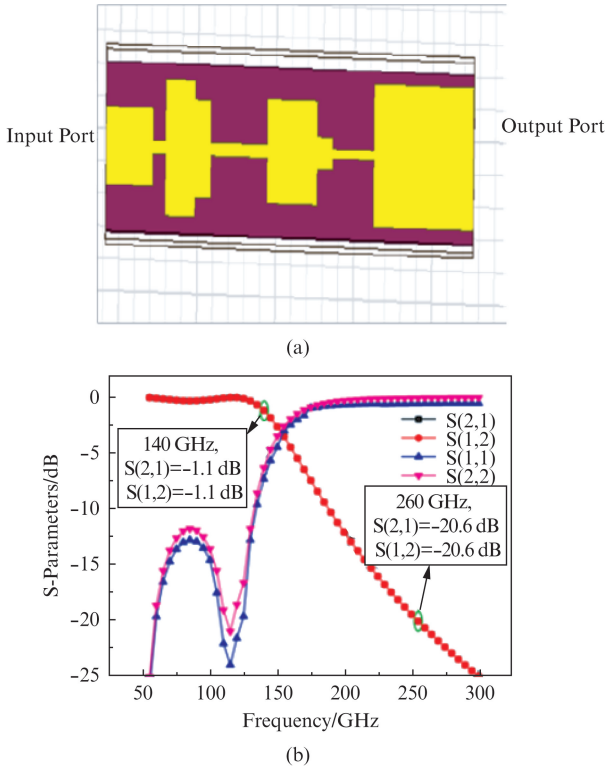

Fig. 6 The structure(a) and simulated result(b) of the low pass filter
图6 (a)低通滤波器结构,(b)仿真结果

50 μm. Waveguide-microstrip transition, lowpass filter is discussed in Sec. 1.2. Input match network is calculated base on the optimal impedance by using linear analysis method. After each part of circuits was optimal individually, the whole detector circuit shown in Fig. 2(b) was analyzed. The S-parmeter file was extracted and then combined with nonlinear diode to optimize the responsivity. This co-simulation process was repeated for further optimization. The optimized simulated responsivity was shown in Fig. 10, which corresponds to input port reflect coefficient(due to the limit of measurement equipment, the input port reflect coefficient can not be measured) shown in Fig. 7. The simulated responsivity is among 1 600 V/W, as the simulated reflect coefficient is under -13dB.

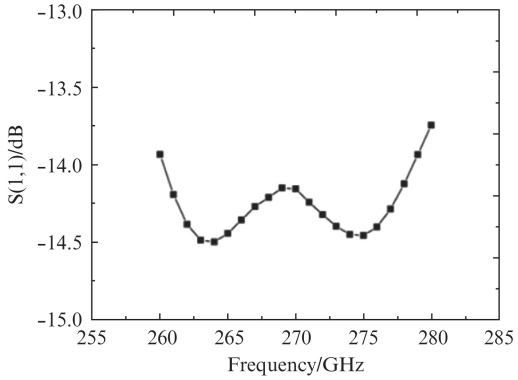

Fig. 7 Simulated input reflect coefficient of the detector
图7 检波器仿真的射频输入反射系数

2 Experimental results

The quartz substrate was mounted to the waveguide block with conductive adhesive. The split block was manufactured by brass and electroplated with 0.5 um gold. The split block photo is shown in Fig. 8. The input port of the detector is standard WR-3 waveguide with dimension of 0.832 mm × 0.416 mm. A SMA connector was used to connect the output port.

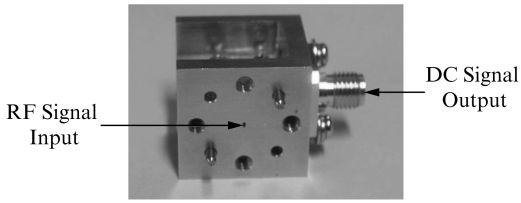

Fig. 8 Photo of the detector
图8 检波器实物照片

2.1 Detector Responsivity Measurement

Figure 9 shows the detector responsivity measurement block diagram. An Agilent microwave source (E8257D) together with a VDI WR3.4 amplified multiplier chain (output power: 0.3 ~ 0.5 mW in 260 ~ 280 GHz) were employed to provide the terahertz power (PRF), which was measured by Erickson power meter. A 20 dB VA3R attenuator was placed between VDI multiplier chain and the detector to keep the input power to the detector in the range from 3 ~ 5 μW. This also insured that the detector was operating in the square-law region[8][9]. The terahertz signal is pulse modulation (PM) modulated (pulse period: 1 mS, pulse width: 0.5 mS). Because the DC output signal from the detector was small, a low noise voltage amplifier (SR560) with gain 100 was placed between the detector and oscilloscope(MSO4104).

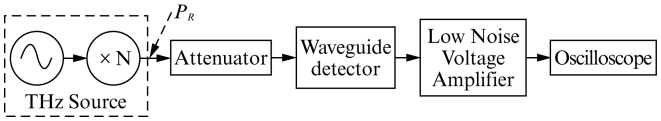

Fig. 9 Diagram of the responsivity measurement setup for detector
图9 检波器电压响应度测试原理图

The responsivity of the waveguide detector is determined by $Rv = (V/100)/(PRF/100) = V/PRF$[10], where V is the peak-peak voltage detected by the oscilloscope, PRF is the incident RF power presented by Erickson power meter. Due to this solution, the responsivity of the waveguide detector is estimated in the range of 1 200 ~ 1 600 V/W while the frequency range from 260 ~ 280 GHz, as shown in Fig. 10. The measured results is much similar to the simulated, although the simulated responsivity is little higher than measured one.

2.2 NEP calculation

When the detector is used to measure small signals, this thermal noise will be the dominant noise source[10].

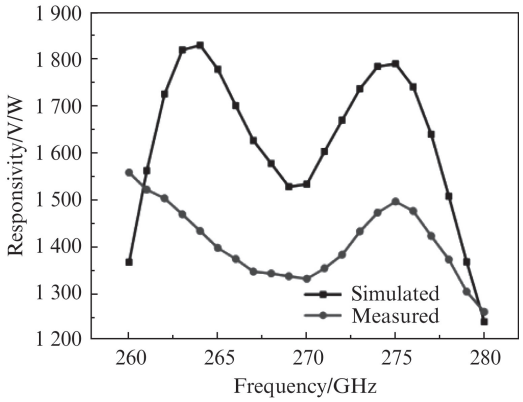

Fig. 10　Measured and simulated responsivity of waveguide
图 10　检波器电压响应度测试和仿真曲线图

The NEP is calculated by[9]

$$NEP = \frac{V_n}{R_v} \quad , \quad (1)$$

where Vn is thermal voltage, Rv is responsivity. The thermal voltage is calculated by[11]

$$V_n = \sqrt{4kBTR} \quad , \quad (2)$$

where k is Boltzmann's constant, T is temperature (degrees Kelvin), B is bandwidth, R is noisy resistance. Noisy resistance is equals the zero-bias junction resistance calculated by

$$R = \frac{dV}{dI} = \frac{V_o}{I_{sat}} \quad , \quad (3)$$

where $Vo = \eta kT/q$, $Isat$ is saturated current, η is ideality factor. Therefore, according to Eqs. (1), (2), and (3), the noise equivalent power is calculated. The calculated NEP of detector is shown in Fig. 11. The NEP is under 20 pW/Hz$^{1/2}$ from 260 ~ 280 GHz and the minimum NEP is near 16.5 pW/Hz$^{1/2}$.

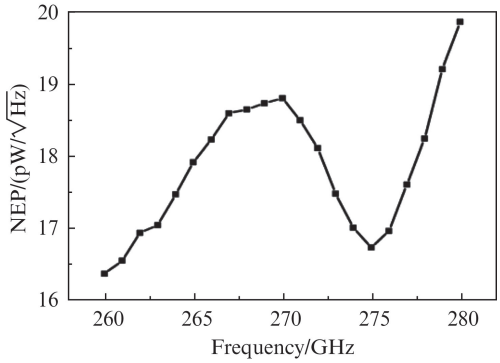

Fig. 11　The calculated NEP of detector
图 11　检波器 NEP 计算曲线图

Compared with commercial waveguide detector products performance which base on InP Schottky diode, the responsivity of this designed detector is a little lower than that of VDI products (VDI represents state-of-the art performance in Terahertz multiplying, mixing and detecting field), and the NEP of proposed detector is bigger than that of VDI products. Moreover, this designed detector was successfully used for imager system, and experiment picture is shown Fig. 12.

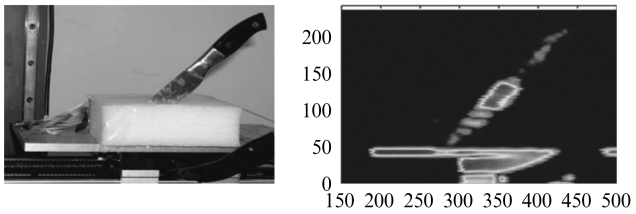

Fig. 12　The experiment picture of the imager system base on the detector
图 12　基于此检波器的成像系统实验图片

3　Conclusions

A 270 GHz waveguide detector was designed, analyzed, simulated and measured based on a zero-bias Schottky diode. It's features using single Schottky diode and the simple circuit topology without direct current (DC) bias supply make it easy and cheap to be fabricated. All passive networks are designed and optimized by HFSS. The performance of entire waveguide detector is analyzed and optimized by ADS. The measured responsivity is above 1 200 V/W from 260 ~ 280 GHz and maximum responsivity is near 1 600 V/W. The NEP is under 20 pW/Hz$^{1/2}$ from 260 ~ 280 GHz and the minimum NEP is near16.5 pW/Hz$^{1/2}$.

The waveguide detector have advantages of simple, compact, low cost and high performance. It is can be used for a variety of applications such as molecular spectroscopy, atmospheric remote sensing, etc. The broadband (220 ~ 330 GHz) waveguide detector is under investigation.

4　Acknowledgement

The authors acknowledge the help of Li Chao and Gao Xiang of Institute of Electronic of Chinese Academy of Sciences for measurement and imaging. Moreover, we appreciate the reviewers and editors for their careful and patient work, and highly improve the quality of this paper.

References

[1] YAO Chang-Fei, ZHOU Ming, LUO Yun-Sheng, *et al*. 150 GHz and 180 GHz fixed-tuned frequency multiplying sources with planar Schottky diodes [J]. *J. Infrared Millim Waves* (姚常飞,周明,罗运生,等. 基于肖特基平面二极管的 150 GHz 和 180 GHz 固定调节式倍频源,**红外与毫米波学报**),2013,**32**(2):102 - 107.

[2] Sun Y F, Sun, J D, Zhou Y, *et al*. Room temperture GaN/AlGaN self-Mixing terahertz detector enhanced by resonant antennas [J]. *Applied Physics Letters*, 2011, 98: 98 - 99.

[3] Sotoodeh M, Khalid A H, Rezazadeh A A. Empirical low-field mobility model for Ⅲ-Ⅴ compounds applicable in device simulation codes [J]. *Appl. Phys*. 2000, **87**(6):2890.

[4] Alexei Semenov, Oleg Cojocari, Heinz-Wilhelm, *et al*. Application of Zero-Bias Quasi-Optical Schottky-Diode detectors for Monitoring Short-Pulse and Weak Terahertz Radiation [J]. *IEEE Electron Device Letters*, 2010, **31**(7): 674 - 676.

[5] Peter Sobis. Advanced Schottky Diode Receiver Front-Ends for Terahertz Applications. [D]. Chalmers University of Technology, Göteborg, Sweden. May 2011.

(下转第 22 页)

References

[1] Rogalski A. Recent progress in infrared detector technologies[J]. *Infrared Phys. Tech.* 2011, **54**(3): 136 - 154.

[2] Gunapala S D, Ting D Z, Hill C J, *et al*. Large area Ⅲ-Ⅴ infrared focal planes[J]. *Infrared Phys. Tech.* 2011, **54**(3): 155 - 163.

[3] Dong Sh, Li N, Chen S H, *et al*. Impact ionization in quantum well infrared photodetectors with different number of periods[J]. *J. Appl. Phys.* 2012, **111**(3): 034504.

[4] Zhai ShQ, Liu JQ, Wang XJ, *et al*. 19 μm quantum cascade infrared photodetectors[J]. *Appl. Phys. Lett.* 2013, **102**(19): 191 - 120.

[5] Rogalski A. Infrared Detectors for the Future[J]. *Acta Phys. Pol. A.* 2009, **116**(3): 389 - 406.

[6] Gunapala S D, Bandara S V, Liu J K, *et al*. Quantum well infrared photodetector research and development at Jet Propulsion Laboratory[J]. *Infrared Phys. Tech.* 2001, **42**(3 - 5): 267 - 282.

[7] Lu W, Li N, Zhen H L, *et al*. Development of an infrared detector: Quantum well infrared photodetector[J]. *Sci. Sin-Phys. Mech. Astron.* (陆卫,李宁,甄红楼,等. **中国科学G辑 物理学 力学 天文学**), 2009, **52**(7): 969 -977.

[8] Li N, Guo F M, Xiong D Y, *et al*. 256times1 very long wavelength QWIP FPAs[J]. *Infrared and Laser Engineering*. (李宁,郭方敏,熊大元,等. **红外与激光工程**), 2006,**35**(6): 756 - 758.

[9] Coon D D, Karunasiri R P G. New mode of IR detection using quantum wells[J]. *Appl. Phys. Lett.* 1984, **45**(6): 649 - 651.

[10] Levine B F, Choi K K, Bethea C G, *et al*. New 10 μm infrared detector using intersubband absorption in resonant tunneling GaAlAs superlattices[J]. *Appl. Phys. Lett.* 1987, **50**(16): 1092 - 1094.

[11] Levine B F, Bethea C G, Choi K K, *et al*. Bound-to-extended state absorption GaAs superlattice transport infrared detectors[J]. *J. Appl. Phys.* 1988, **64**(3): 1591 - 1593.

[12] Steele A G, Liu H C, Buchanan M, *et al*. Importance of the upper state position in the performance of quantum well intersubband infrared detectors[J]. *Appl. Phys. Lett.* 1991, **59**(27): 3625 - 3627.

[13] Levine B F, Zussman A, Gunapala S D, *et al*. Photoexcited escape probability, optical gain, and noise in quantum well infrared photodetectors[J]. *J. Appl. Phys*, 1992, **72**(9): 4429 - 4443.

[14] Gunapala S D, Park J S, Sarusi G, *et al*. 15-μm 128 × 128 GaAs/$Al_xGa_{1-x}As$ quantum well infrared photodetector focal plane array camera[J]. *IEEETrans. on Electron Devices*, 1997, **44**(1): 45 - 50.

[15] Gunapala S D, Liu J K, Park J S, *et al*. 9-μm cutoff 256 ×256 GaAs/$Al_xGa_{1-x}As$ quantum well infrared photodetector hand-held camera[J]. *IEEETrans. on Electron Devices*, 1997, **44**(1): 51 - 57.

[16] Schneider H, Liu H C. *Quantum Well Infrared Photodetectors: Physics and Applications*[M]. NewYork: Springer, 2007.

[17] Gunapala S D, Bandara KM S V, Levine B F, *et al*. High performance InGaAs/GaAs quantum well infrared photodetectors[J]. *Appl. Phys. Lett*, 1994, **64**(25): 3431 - 3433.

[18] Panand J L, Fonstad Jr C G. Theory, fabrication and characterization of quantum well infrared photodetectors[J]. *Materials Science and Engineering Reports*, 2000, **28**(3 - 4): 65 - 147.

[19] Chang W H, Hsu T M, Huang C C, *et al*. Photocurrent studies of the carrier escape process from InAs self-assembled quantum dots[J]. *Phys. Rev. B*, 2000, **62**(11): 6959 - 6962.

[20] Gonschorek M, Schmidt H, Bauer J, *et al*. Thermally assisted tunneling processes in $In_xGa_{1-x}As$/GaAs quantum-dot structures[J]. *Phys. Rev. B*, 2006, **74**(11): 115312 (1 - 13).

[21] Fu Y, Lu W. *Physics of Semiconductor Quantum Devices*[M]. Beijing: Science Press(傅英,陆卫. **半导体量子器件物理**. 北京: 科学出版社),2005.

[22] Vurgaftman I, Meyer J R, Ram-MohanL R. Band parameters for Ⅲ-Ⅴ compound semiconductors and their alloys[J]. *J. Appl. Phys.*, 2001,**89**(11): 5815 - 5875.

(上接5页)

[6] Hesler J L. Planar Schottky Diodes in Submillimeter-Wavelength Waveguide Receivers.[D]. School of Engineering and Applied Science, University of Virginia, Charlottesville, United States, 1996.

[7] Tang A. Y. Modelling of terahertz planar schottky diodes.[D]. Department of Microtechnology and Nanoscience, Chalmers University of Technology, Göteborg, Sweden, 2011.

[8] Jeffrey L Hesler, Thomas W Crowe. NEP and Responsivity of THz Zero-Bias Schottky Diode Detectors[C]. Infrared and Millimeter Waves, 2007 and the 2007 15th International Conference on the Terahertz Electronics: 844 - 845.

[9] Jeffrey L. Hesler, Thomas W. Crowe. Responsivity and Noise Measurements of Zero-Bias Schottky Diode Detector[C]. 18th Intl. Symp. Space Terahertz Techn., Pasadena, March 2007.

[10] Lei Liu, Jeffrey L. Hesler, Haiyong Xu, *et al*. A Broadband Quasi-Optical Terahertz Detector Utilizing a Zero Bias Schottky Diode [J]. *IEEE Microwave and Wireless Components Letters*, 2010, **20**(9):504 - 506.

[11] David M Pozar *Microwave Engineering* (*Third Edition*)[M]. Beijing: Publishing House of Electronic Industry(波扎,**微波工程(第三版)**. 北京:电子工业出版社),2007.